Investigations of Ion Channel Structure-Function Relationships Using Molecular Modeling and Experimental Biochemistry

Thesis by

Donald Eugene Elmore, Jr.

In Partial Fulfillment of the

Requirements for the Degree of

Doctor of Philosophy

California Institute of Technology

Pasadena, California

2004

(Defended April 22, 2004)

Chapter 6: Identification of the Mechanosensitive Channel of Small Conductance (MscS) Voltage Sensor

Background

The past few chapters have focused on the mechanosensitive channel of large conductance (MscL), one of three bacterial mechanosensitve channels that have been characterized electrophysiologically. The other two channels, the mechanosensitive channel of small conductance (MscS) (Martinac et al., 1987) and the mechanosensitive channel of miniture conductance (MscM) (Berrier et al., 1989) were originally noted in electrophysiological traces of *E. coli* spheroplasts. Although the gene for MscM still has not been identified, the *E. coli* gene related to MscS activity was cloned by the Booth group in 1999 (Levina et al., 1999). This yggB gene product, which has orthologues in several different bacterial species, shares relatively little sequence homology with MscL. Sequence analyses and PhoA fusion studies predicted that MscS had a more complicated topology than MscL with three transmembrane domains and a sizable C-terminal intracellular region that appears to be necessary for proper channel function (Miller et al., 2003a).

Electrophysiological measurements on MscS also showed important differences between it and MscL. First, measurements of MscS activity before its cloning implied that, in addition to being gated by membrane tension, its activity was notably modulated by changes in transmembrane potential (Martinac et al., 1987). However, this result has not been replicated in the literature after the cloning of MscL. Secondly, in contrast to the non-selective pore of MscL, MscS appears to show a slight selectivity for anions over cations (Sukharev, 2002).

Recently, a 3.9 Å resolution crystal structure of *E. coli* MscS was solved by the Rees group (Bass et al., 2002). This structure confirmed many of the earlier postulations

about the channel topology (Levina et al., 1999; Miller et al., 2003a), and showed the full channel to be a homoheptamer (Fig. 6.1). In addition to having this unique channel symmetry, the MscS structure was also interesting since it appeared to capture the channel as an open conformation instead of the closed conformation observed in the previous structures of MscL (Chang et al., 1998) and other ion channels (Doyle et al., 1998; Dutzler et al., 2002; Jiang et al., 2003a). Although there has been some debate about whether this structure is actually the open state of MscS (Anishkin and Sukharev, In press), results discussed below clearly support the assertion that it minimally represents a conductive state of the channel.

Figure 6.1: The MscS crystal structure. A) A side view of the channel showing secondary structure. Each of the seven homomeric subunits is shown in a different color. B) A top view of the channel in CPK looking from the extracellular side. As in (A), each subunit is shown in a different color. C) A single subunit of MscS with the TM1, TM2, and TM3 regions shown in red, blue, and green, respectively.

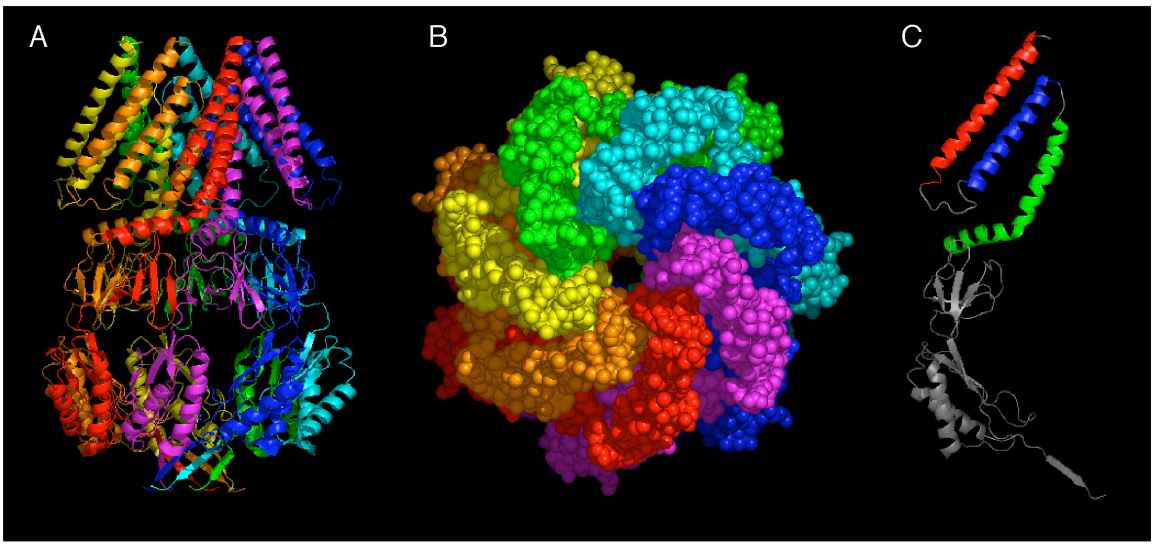

This intriguing channel structure provides the opportunity to consider interesting properties of MscS, such as its voltage sensitivity, on the molecular level. In particular, we can use molecular dynamics (MD) simulations to predict which particular amino acid residues imbue the channel with its voltage sensitivity. The crystal structure has two arginine residues, R46 and R74, in the middle of the transmembrane regions (Fig. 6.2A) that are hypothesized to contribute to the voltage sensitivity (Bass et al., 2002), but other transmembrane charged residues could also be important in this phenomenon. In light of the recent crystal structure of another channel sensitive to transmembrane potential, KvAP, these results on MscS should help refine our ideas about structural aspects of voltage sensitivity (Jiang et al., 2003a).

Setup of Molecular Dynamics Simulations

Residues Tyr 27-179 from the *E. coli* MscS crystal structure (Bass et al., 2002) were used as a starting structure for all simulations, which included all TM domains and the middle-β domain in the simulations (Fig. 6.2A). The C-terminal region after residue 179 was omitted to maintain a reasonable simulation size, although some recent results imply that region may play a role in MscS assembly and/or function (Miller et al., 2003a). All ionizable residues (Asp, Glu, Lys, and Arg; no His are present in the structure) were charged unless specifically noted otherwise, while the N- and C-termini were left uncharged as they do not represent physiological termini of the channel.

Figure 6.2: A) Crystal structure of MscS with the region included in the simulation shown in white and the region omitted in gray. Two arginines, Arg 46 and Arg 74, hypothesized to be important for voltage sensitivity are shown in blue and violet CPK, respectively. B) The embedded MscS system used for MD simulations. The protein is shown as white ribbons, with explicit lipid and water shown as green and blue wireframe, respectively. The phosphorous atoms of lipid headgroups are shown in yellow CPK.

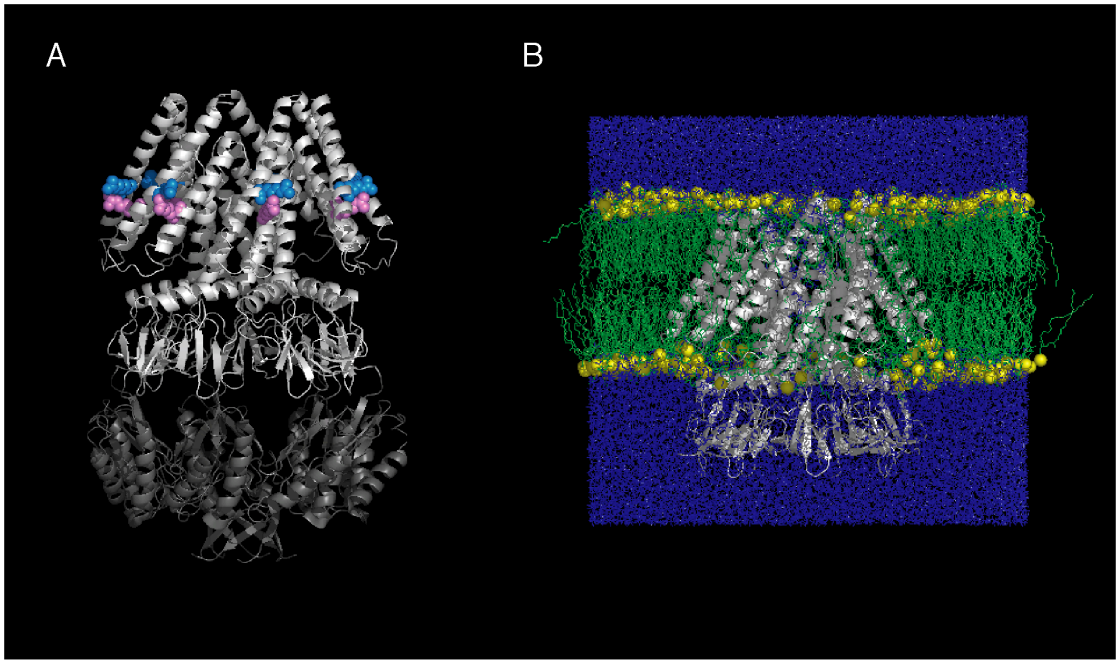

This structure was embedded into an equilibrated membrane of 512 POPE (palmitoyloleoylphosphatidylethanolamine) lipids. Throughout, the membrane was oriented in the *xy* plane, with the *z*-axis as the membrane normal. The membrane used in simulations was created by first converting a 128 POPC (palmitoyloleoyl-phosphatidylcholine) membrane created by Tieleman and co-workers (Tieleman et al., 1999) to POPE, in an analogous manner to POPE to POPC conversions described in Chapter 5. After conversion to POPE, the membrane was equilibrated for 3 ns. This equilibrated 128 POPE membrane was then copied in the *xy* plane to yield a membrane patch of 512 lipids. This enlarged membrane system was equilibrated by MD for an

additional 2 ns. The parameters described below were also used for these membrane equilibration steps.

The MscS channel was embedded into the 512 POPE membrane utilizing methods developed by Faraldo-Gómez et al. (Faraldo-Gomez et al., 2002). Briefly, lipids were removed from each leaflet of the bilayer based on the exclusion volume of the channel structure calculated using MSMS (Sanner et al., 1996); 53 total lipids were removed during this step. Then, the remaining lipids were subjected to forces based on the shape of the channel protein over three short MD simulations, forming a cavity in the membrane in the shape of MscS. These simulations were: a) a 20 ps simulation heating from 5 K to 310 K, with an outward force of 10 kJ/mol Å; b) a 20 ps simulation at 310 K with an outward force of 10 kJ/mol Å; c) a 10 ps simulation at 310 K with an outward force of 100 kJ/mol Å. The channel was then inserted into this cavity, additional waters were added to fully solvate the channel structure, and the system was subjected to 50 steps of steepest descents minimization. Afterwards, 52 Cl^- and 10 Na^+ ions were added based on the electrostatic potential of the system to neutralize the overall system charge, and four lipids which still had significant overlap with the channel were removed. This system was again minimized for 50 steps. The final system included 1071 protein residues, 455 POPE, and 28423 waters for a total of 118,665 atoms, and was about 11.6 nm x 12.2 nm x 10.9 nm. The embedded system is shown in Fig. 6.2B.

The minimized MscS system was heated to 310 K over 20 ps, with restraints on all Cα atoms of the protein structure. These restraints were maintained for an additional 180 ps of MD, after which they were gradually reduced stepwise over an additional 330 ps. This system was then used to begin three different MD simulations.

The first simulation continued the trajectory for an additional 4470 ps, for a total 5 ns of simulation. A second simulation was performed identically to the first except that a potential of 0.1 V/nm (about a 350 mV transmembrane potential) was applied normal to the membrane (in the *z*-direction) during the simulation using a method described by Tieleman, Sansom, and co-workers (Tieleman et al., 2001). This simulation was extended for 6970 ps, for a total trajectory of 7.5 ns. A third simulation was performed with two putative MscS voltage sensing residues, Arg 46 and 74, neutralized and the 0.1 V/nm potential applied throughout. Because of the change in side chain charge states, 14 waters were replaced with Cl^- ions, based on electrostatic potential, to neutralize the overall system. This simulation was extended for 4470 ps, for a total 5 ns of simulation.

All minimizations and MD simulations were performed using the GROMACS 3 suite of programs (Berendsen et al., 1995; Lindahl et al., 2001). The protocols for MD used in this study were analogous to those used in our previous simulations of the Tb-MscL channel (Elmore and Dougherty, 2001; Elmore and Dougherty, 2003). Lipid parameters were from (Berger et al., 1997), with additional parameters for the oleoyl double bond taken from the GROMOS force field. GROMACS atomic parameters were used for protein and water. All MD runs used a time step of 2 fs along with the LINCS routine to constrain bond lengths (Hess et al., 1997) and SETTLE to constrain rigid water geometries (Miyamoto and Kollman, 1992). Long-range electrostatics were computed using PME (Darden et al., 1993), with a Fourier grid spacing of 0.10 nm and cubic interpolation. A 1.0 nm cutoff was employed for Lennard-Jones and real-space Coulombic interactions. Structures from the trajectories were stored every 0.5 ps for analysis. The NPT ensemble was employed with anisotropic pressure coupling in each

direction to 1 bar with a time constant (τ_p) of 1.0 ps (Berendsen et al., 1984). Temperatures were coupled separately for protein, lipid, and solvent to a temperature bath with a coupling constant (τ) of 0.1 ps (Berendsen et al., 1984).

Analyses of trajectories were performed primarily using tools provided in the GROMACS suite, and pore radii were calculated with HOLE (Smart et al., 1997). Structural pictures were created with Pymol (DeLano, W. L., http://www.pymol.org) and Rasmol (Sayle and Milner-White, 1995).

The Channel Structure is Sensitive to Transmembrane Potential in Simulations

In general, the MscS channel is well behaved in MD simulations. As in simulations of MscL and other ion channels, the channel structure initially shows some drift from the crystal structure—as would be expected for a structure at only 3.9 Å resolution—but generally seems to equilibrate within the constraints of the simulation (Fig. 6.3). However, in the absence of any transmembrane voltage, the channel adjusts fairly rapidly to form an occlusion across the pore region through which water cannot pass (Fig. 6.4). The occlusion does not require a large conformational shift in the channel structure, but instead occurs as a few of the TM3 helices adjust in an asymmetric manner to use the L105 and L109 residues, which form the narrowest constriction in the crystal structure, to form the occlusion (Fig. 6.5). Once it appears, the occlusion remains across the pore throughout the rest of the 5 ns simulation. Since this occlusion occurs so quickly in the simulation, and these simulations are constrained to relatively short nanosecond timescales, we are hesitant to refer to this as the "closed" state of the channel. In addition, this occluded conformation does not agree fully with cross-linking data obtained

on MscS channel thought to be in the closed state (Miller et al., 2003b). Regardless, the TM motions that led to the occlusion provide an intriguing starting point for thinking about channel closure as a potentially asymmetric process, and the rapid collapse of the channel into an occluded state shows the instability of the crystal structure conformation in the absence of some applied stimulus, such as a transmembrane potential.

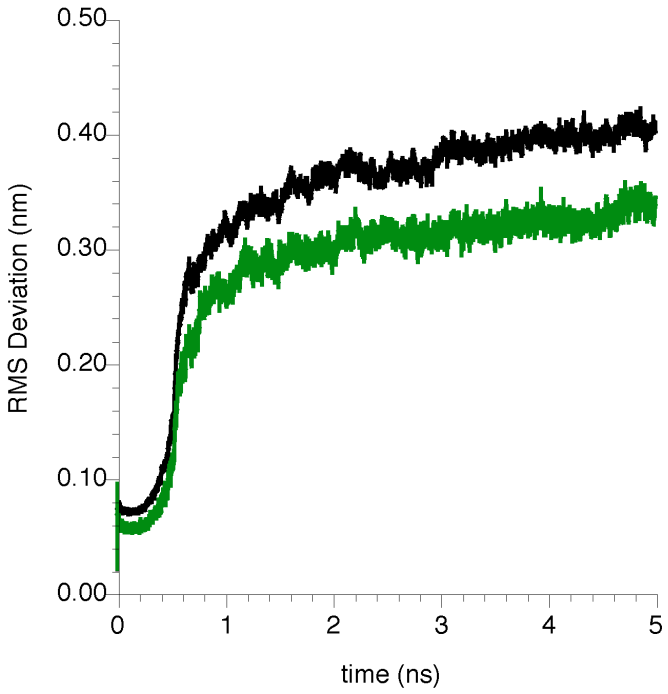

Figure 6.3: RMS deviation from crystal structure in the MscS simulation with no applied voltage. These values were calculated for all Cα in the protein (black) or just Cα in the pore-lining TM3 domain (green) for each frame of the simulation by first fitting all protein Cα to the crystal structure.

Since MscS is thought to be a voltage-sensitive channel, we performed a simulation in which a 0.1 V/nm voltage was applied across the simulation box. This corresponds to a 300-400 mV transmembrane potential, which although higher than that typically observed in living cells is in the range used in previous simulations (Robertson and Tieleman, 2002; Tieleman et al., 2001) and would be feasible for electrophysiological studies. In particular, simulations performed by Tieleman and co-

workers have shown that the membrane models used here are stable under this magnitude of applied voltage.

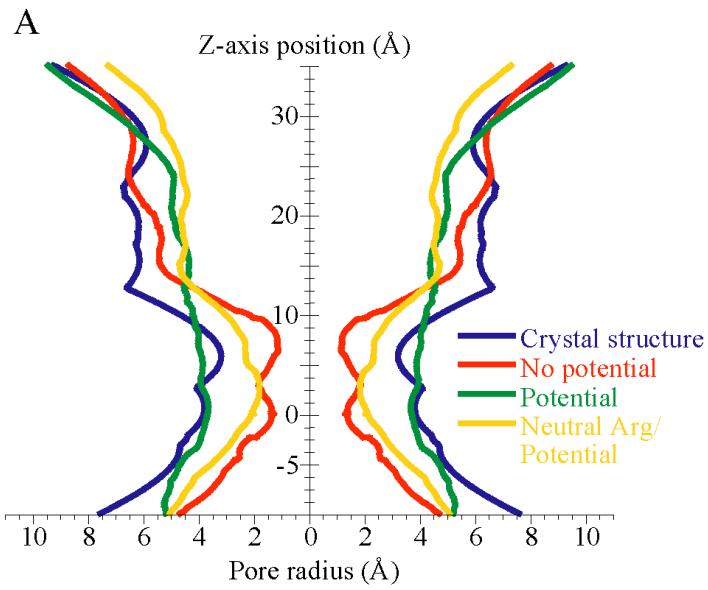

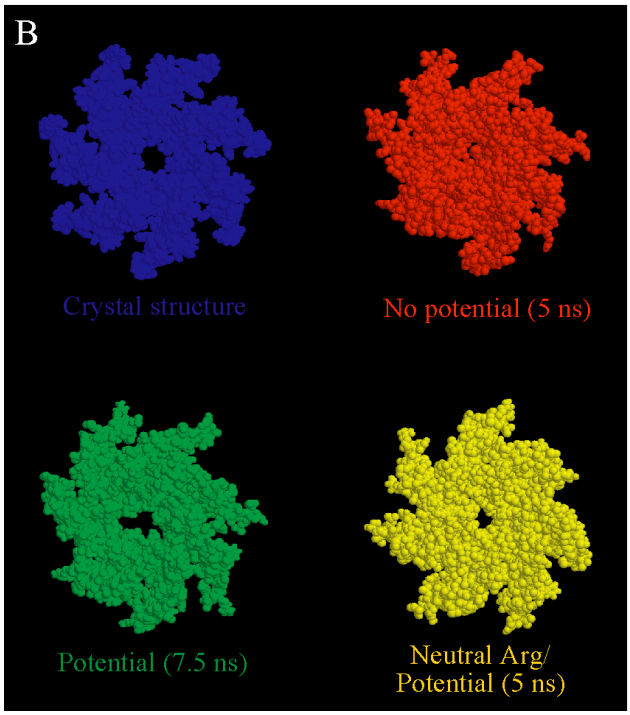

Figure 6.4: A) Plot showing the radius along the MscS pore calculated using HOLE. Radii for simulations were averaged over frames taken every 50 ps over the final 250 ps of each trajectory. The Z-axis position refers to position along the membrane normal, with 0 set at the position of L109. B) CPK pictures of the MscS crystal structure and the final frame of different trajectories. Each picture is oriented looking from the extracellular side of the channel and includes only TM residues for clarity.

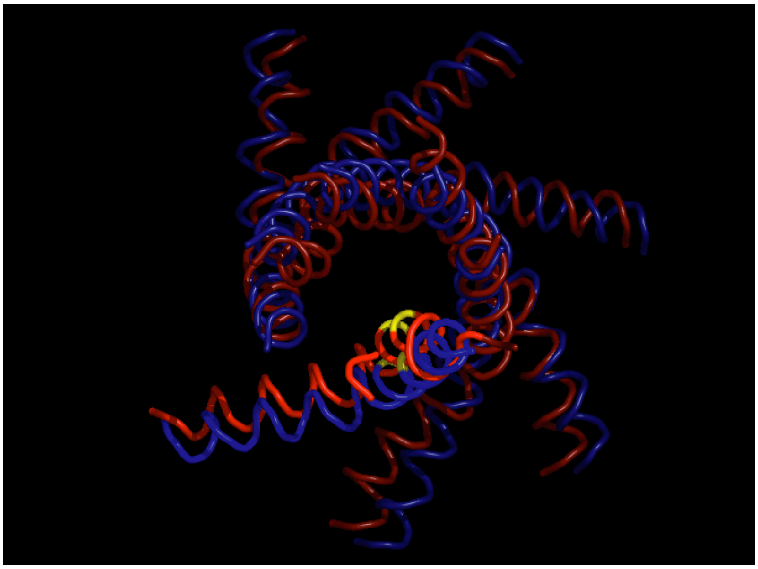

Figure 6.5: Superimposed TM3 regions from the crystal structure (blue) and the 5 ns frame of the simulation with no applied voltage (red). The subunit in brighter colors was one that moved such that the L105 and L109 (shown in yellow) residues occluded the channel. The TM3 of one subunit is omitted for clarity.

Interestingly, the channel does *not* relax into the occluded state in this simulation with an applied voltage (Fig. 6.4). In fact, the channel never becomes more occluded than the crystal structure throughout a 7.5 ns trajectory. It appears that the non-occluded conformation seen in the crystal structure is stabilized by applied voltage, while that conformation is unstable if such a voltage is not applied. Thus, the channel structure is clearly sensitive to transmembrane potentials.

Remarkably, the occluded channel from the simulation can also be "reopened" by an applied voltage. When the 5 ns occluded final frame from the simulation with no voltage applied was subjected to a potential of 0.33 V/nm across the box, the occlusion was removed from the channel. Interestingly, this "reopening" did not occur within a few ns when the channel was only subjected to the 0.1 V/nm voltage used to maintain the non-occluded state.

Does the Crystal Structure Represent an "Open" State?

As mentioned earlier, there has been some debate about whether or not the MscS crystal structure represents an open state of the ion channel. Initially, Bass et al. felt that the relatively wide diameter of the MscS pore in the structure (≈ 11 Å at its narrowest point) implied the structure was in the open state (2002). However, recent MD simulations by Anishkin and Sukharev (in press) have implied that the most constricted region of the crystal structure pore is so hydrophobic that it would expel water and induce a "vapor-lock" that effectively blocks the channel to ion passage.

Our MD simulations show that this pore "dewetting" behavior is likely an artifact of a simulation that was not allowed to equilibrate fully (Anishkin and Sukharev, In press). In order to increase computational efficiency, Anishkin and Sukharev included only fragments of the MscS TM regions in their simulations. Thus, in order to maintain a reasonable conformation, they placed restraints on the backbones of the TM regions. In their trajectory, water is rapidly expelled from the most constricted region of the pore and generally does not reenter during the remainder of a 6 ns simulation.

We also observe a similar "dewetting" phenomenon in the initial *nonequilibrated* portion of our MD simulations in which the channel is subjected to restraints. During this early portion of the trajectory, the majority of water molecules leave the constricted region of the pore, and in some frames, such as at 250 ps (Fig. 6.6A), there is a clear region devoid of water. However, in the voltage applied simulation where the channel does not become occluded, water rapidly reenters the pore after the restraints are fully released from the system, and there is a clear column of water through the channel that remains throughout the full 7.5 ns simulation (Fig. 6.6B and C). In fact, many ions pass

through this region of the pore over the course of the trajectory. Thus, in our *equilibrated* system there is no evidence that the channel pore is blocked to the passage of ions by a region devoid of water.

Figure 6.6: Pictures of the 250 ps (A), 2 ns (B), and 7.5 ns (C) frames from the simulation with 0.1 V/nm potential applied (no potential was applied yet at 250 ps).

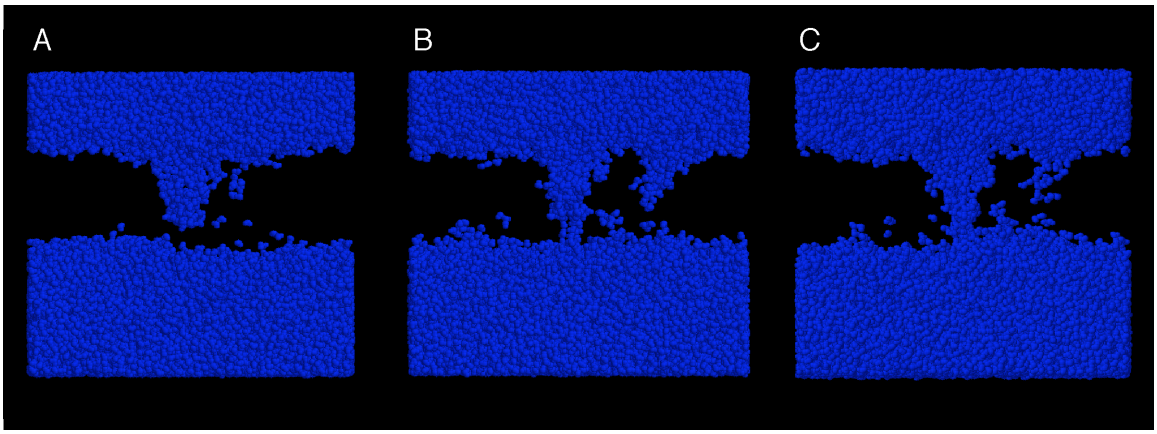

This might lead one to wonder whether the pore region conformation of the channel changes significantly in our simulation to allow the reentry of water. The most notable change upon the release of restraints is a break of symmetry in the pore region (Fig. 6.7 A). In breaking this symmetry, the TM3 helices are able to present a somewhat less hydrophobic face to the pore, promoting the reentry of water into the pore. In addition, some of the polar side chains of Q112 residues move up towards the L105/L109 constriction as the simulation progresses, further stabilizing water in the region (Fig. 6.7B). However, these conformational changes are relatively minor. The experimental structure was only solved to 3.9 Å resolution, and the RMS deviation of all TM3 atoms from the crystal structure is just about 3 Å at the point in the trajectory where water

reenters the pore, and it hits a maximum of about 4 Å throughout the 7.5 ns trajectory. As well, the perfect heptameric symmetry imposed during the solving of the crystal structure would almost certainly not exist at any moment in time in a physiological system. In general, it seems very reasonable from an energetic standpoint that the channel protein would experience these relatively conservative changes to eliminate an effective vacuum within the pore.

Interestingly, an ongoing collaboration between the Roux group and ourselves using Brownian Dynamics simulations and electrostatic calculations (Im et al., 2000) to predict MscS conductance based on the crystal structure implies that the crystal structure represents a conductive state of the channel (unpublished data). These predictions are still preliminary, and it is unclear from them whether the structure actually represents a *conductive* intermediate state or the fully open state of the channel. However, these models clearly do not imply that the MscS crystal structure represents a non-conductive state of the channel. Thus, throughout the rest of this chapter the conformation of MscS in simulations with an applied voltage will be referred to as the "conductive" state.

Figure 6.7: Top (A) and side (B) views of TM3 regions from the 250 ps (left) and 2 ns (right) frames from an MscS trajectory. The 2 ns frame is taken from a trajectory with 0.1 V/nm voltage applied to the system. L105 and L109 are shown in yellow CPK, and Q112 is shown in blue CPK.

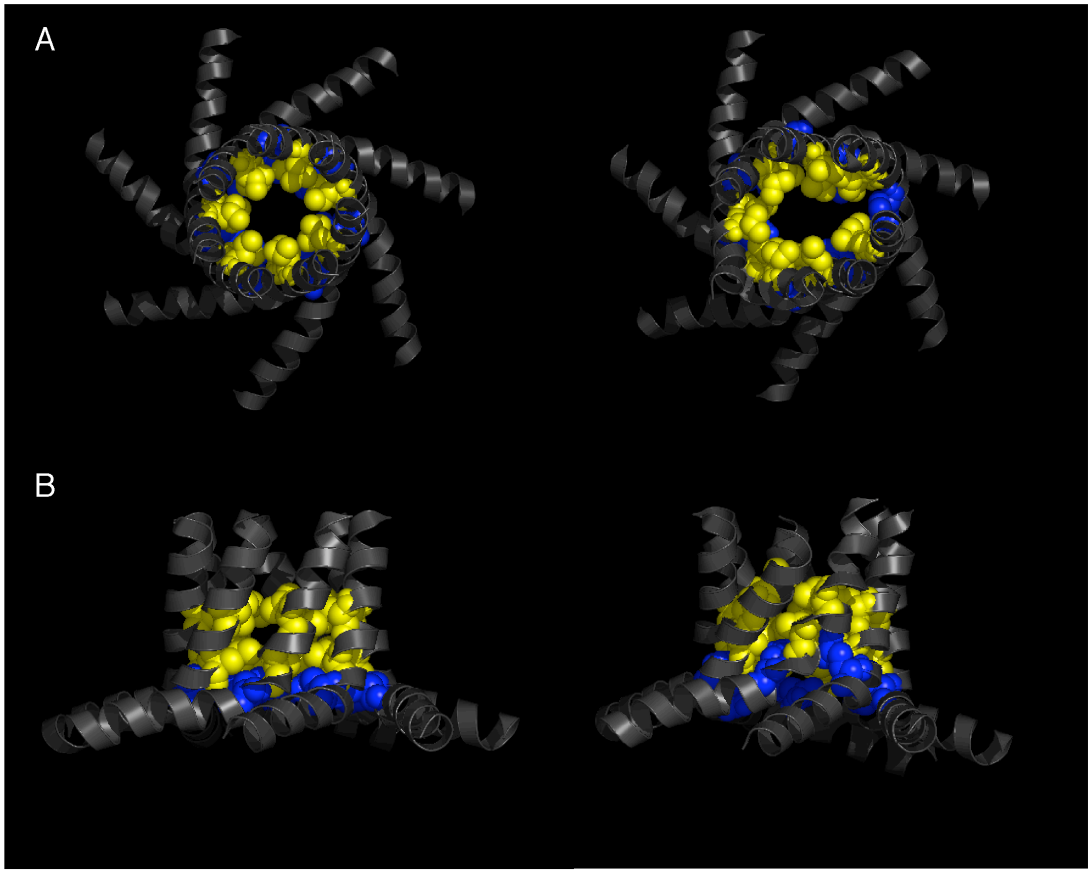

What Chemical Moieties Give the Channel Its Voltage Sensitivity?

The conventional model of voltage sensitivity implies that a voltage-sensitive channel has charged residues that move through the transmembrane region—and thus the transmembrane potential field—as the channel progresses from its open to closed conformations (Hille, 2001). We observed this type of behavior in the MD simulation in which MscS moves from its conductive conformation to the occluded conformation. In

particular, we initially noted that the two arginines originally considered to be voltage sensor residues, R46 and R74, dropped significantly towards the intracellular side of the membrane in the occluded trajectory (Fig. 6.8). Conversely, these residues maintained their relative transmembrane position throughout the simulation with an applied voltage.

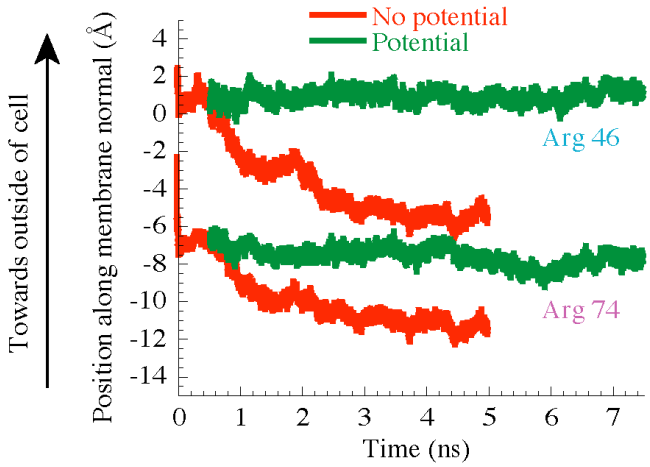

Figure 6.8: Position of R46 and R74 residues in simulations with and without applied potential. Positions were taken as the position of the □-carbon of the arginine residue, which is the charge center of the side chain. The zero position on the membrane normal is set at the center of the membrane.

These results implied that those residues might be important in providing MscS with its voltage sensitivity. To test this assertion, we performed an additional simulation of MscS in which R46 and R74 were changed to their neutral form. In this simulation, the channel became quite occluded even in the presence of the 0.1 V/nm potential field that maintains the wild-type channel in its conductive state (Fig. 6.4). Interestingly, the channel did not become fully occluded to the extent seen in the simulation without an applied voltage over this 5 ns simulation. Thus, it appeared that while R46 and R74 provide the channel with most of its voltage sensitivity, other residues that are still charged in this simulation also may play a role in sensing transmembrane potentials. As expected, a simulation of MscS with R46 and R74 neutralized that did not have an applied potential rapidly progressed towards the fully occluded state.

Another simulation with an R46A mutation and an applied 0.1 V/nm potential also was performed to further confirm this result (S. A. Spronk, unpublished results). This simulation is more directly comparable to conventional experimental mutagenesis of the channel converting an arginine residue to an alanine. R46 was chosen as the initial target over R74 since it showed a larger movement in the non-voltage applied simulation (Fig. 6.8), implying that it is likely more important for voltage sensitivity. The results of the R46A simulation were qualitatively identical to those of the neutralized R46/R74 simulation (data not shown).

Table 6.1: Positions and relative movement along the membrane normal (*z*-axis) of charged TM residues in MscS trajectories with (conductive state) and without (occluded state) 0.1 V/nm applied potential. Positions are averaged over the final 1 ns of each trajectory and expressed such that zero is the membrane center and increasingly positive positions are towards the periplasmic side of the membrane. Relative changes are expressed such that positive values represent movement towards the cytoplasmic side in the simulation without applied potential.

Residue	Position in Trajectory with Applied Potential	Position in Trajectory without Applied Potential	Relative Change in Position Towards Cytoplasmic Side
R46	1.2 Å	-5.5 Å	6.7 Å
R54	-11.4 Å	-14.5 Å	3.1 Å
D67	-12.6 Å	-15.5 Å	2.9 Å
R74	-7.8 Å	-11.3 Å	3.5 Å
R88	11.1 Å	7.5 Å	3.6 Å

However, both the neutralized R46/R74 and R46A simulations do not show complete channel occlusion, implying that other charged residues in the transmembrane region may contribute to the voltage sensitivity of MscS. In fact, other charged residues show movement equivalent to that of R74 as the channel progresses from the conductive

to occluded states (Table 6.1). This includes two other positively charged arginines (R54 and R88) and one negatively charged aspartate (D67) that move towards the intracellular region. Thus, R54 and R88 would help promote voltage sensitivity, while D67 would actually oppose it. Together with R46 and R74, the motion of these residues implies that the transition between the conductive and occluded states would involve a motion of : 7 * (6.7 + 3.1 – 2.9 + 3.5 + 3.6) = 98 charge•Å. Assuming a membrane thickness of 35 Å, this corresponds to 2.8 charges moving across the membrane during the transition.

Agreement with Experimental Electrophysiology

Preliminary electrophysiological results on wild-type and R46A MscS expressed in *E. coli* spheroplasts generally agree with the predictions from MD simulations described above (L. W. Lee, unpublished data). Wild-type MscS does show voltage modulation, with an e-fold change in its open probability for every 6.44 mV of transmembrane potential at a constant applied tension. This is a somewhat greater voltage sensitivity than the previously observed e-fold increase in open probability for every 15 mV of transmembrane potential (Martinac et al., 1987). These experimentally measured voltage sensitivities can be compared to the 2.8 charge equivalents moving across the membrane as the channel transitions between the conductive and occluded states found in MD simulations. The e-fold increase for 15 mV would imply the motion of 1.6 charges across the membrane, while the e-fold increase for 6.44 mV implies a motion of 3.7 charges across the membrane. Although the movement of 2.8 charges across the membrane in our simulations is between these two numbers, it does imply that previous studies may have underestimated the voltage sensitivity of the channel.

As well, the R46A channel shows essentially no sensitivity to transmembrane potential in electrophysiological measurements, again supporting its predicted importance in providing a significant portion of the channel's voltage sensitivity. Unfortunately, attempts to experimentally characterize an R74A mutant have been hampered by the apparently poor expression of that channel in *E. coli* spheroplasts, but future attempts to characterize the sterically subtler but still uncharged R74Q mutant will hopefully provide interesting results.

Discussion

Molecular dynamics simulations have proven to be a very useful tool to structurally consider the voltage modulation of MscS, predicting specific amino acid residues that give the channel its voltage sensitivity. In particular, it appears that R46 is a central residue for giving the channel its ability to respond to transmembrane potentials. However, the MD simulations also imply that other charged residues in the MscS TM regions may be important in voltage sensing mechanisms, and additional simulations and experimental characterizations of MscS mutants can further investigate these possibilities.

The voltage sensing in MscS has both interesting similarities and differences to the voltage sensing "paddle" proposed for KvAP (Jiang et al., 2003a; Jiang et al., 2003b). Like the voltage paddle, many of the MscS residues that appear to respond to transmembrane potential, particularly R46, face the lipid membrane. However, the voltage sensing regions move much less dramatically in MscS, although this may be partially due to its lower sensitivity to voltage. Also, if other charged residues, such as

R88, do play a significant role in MscS voltage sensitivity, then the voltage sensing residues are also less concentrated in a single substructure in MscS.

Future investigations on MscS should probe in more detail how force is transduced between the MscS TM regions in order to couple the motion of the TM1 and TM2 regions that contain the voltage sensing residues—and also would directly sense tension applied through the membrane—and the pore-lining TM3 region. In particular, MD simulations could be used to calculate interaction energies between residues in the TM regions, and the importance of residues with significant interactions could then be probed by experimental mutagenesis. These mutants could be characterized by electrophysiology, but it might be more efficient to characterize a larger set of mutations by adapting the high-throughput assay used to characterize MscL mutants (Maurer and Dougherty, 2001) to MscS. The high-throughput assay should be appropriate for MscS since Miller et al. (2003) were able to characterize MscS mutants using standard growth-based assays. This approach combining interaction energies from MD simulations and experimental mutagenic analyses is similar to that described in Chapter 5 and in (Elmore and Dougherty, 2003) for determining that lipid-interacting residues are more important than intersubunit interactions for MscL function. In addition, since MscS is a mechanosensitive channel like MscL, it would also be interesting to determine whether its residues that interact strongly with lipid are also critical for proper channel function.

It would also be valuable to focus on the potential role of the extensive intracellular C-terminal domains of MscS. Even minor cleavages in the C-terminal region lead to a channel that cannot effectively rescue bacteria from osmotic downshock (Miller et al., 2003a). Although it is unclear whether this dramatic loss of channel

function results from improper channel assembly or a properly assembled but non-functional channel, it is clear that even the most distal portion of the intracellular domain plays some critical role in MscS structure or function. Other work has shown that the intracellular domains of the channel appear to rearrange their conformation upon channel gating, since binding of a C-terminal hexa-histidine tag to metal ions prevents closed channels from opening (Koprowski and Kubalski, 2003). Thus, future simulations should aim to include this full region from the crystal structure.

References

Anishkin, A., and S. Sukharev. In press. Water dynamics and dewetting transitions in the small mechanosensitive channel MscS. *Biophys. J.*

Bass, R. B., P. Strop, M. Barclay, and D. C. Rees. 2002. Crystal structure of *Escherichia coli* MscS, a voltage-modulated and mechanosensitive channel. *Science* 298:1582-7.

Berendsen, H. J. C., J. P. M. Postma, W. F. van Gunsteren, A. DiNola, and J. R. Haak. 1984. Molecular dynamics with coupling to an external bath. *J. Chem. Phys.* 81:3684-3690.

Berendsen, H. J. C., D. van der Spoel, and R. van Drunen. 1995. GROMACS: A message-passing parallel molecular dynamics implementation. *Comp. Phys. Comm.* 91:43-56.

Berger, O., O. Edholm, and F. Jähnig. 1997. Molecular dynamics simulations of a fluid bilayer of dipalmitoylphosphatidylcholine at full hydration, constant pressure, and constant temperature. *Biophys. J.* 72:2002-2013.

Berrier, C., A. Coulombe, C. Houssin, and A. Ghazi. 1989. A patch-clamp study of ion channels of inner and outer membranes and of contact zones of *E. coli*, fused into giant liposomes. Pressure-activated channels are located in the inner membrane. *FEBS Lett.* 259:27-32.

Chang, G., R. H. Spencer, A. T. Lee, M. T. Barclay, and D. C. Rees. 1998. Structure of the MscL homolog from *Mycobacterium tuberculosis*: a gated mechanosensitive ion channel. *Science* 282:2220-6.

Darden, T. D., D. York, and L. Pedersen. 1993. Particle mesh Ewald: An N log(N) method for Ewald sums in large systems. *J. Chem. Phys.* 98:10089-10092.

Doyle, D. A., J. Morais Cabral, R. A. Pfuetzner, A. Kuo, J. M. Gulbis, S. L. Cohen, B. T. Chait, and R. MacKinnon. 1998. The structure of the potassium channel: molecular basis of K^+ conduction and selectivity. *Science* 280:69-77.

Dutzler, R., E. B. Campbell, M. Cadene, B. T. Chait, and R. MacKinnon. 2002. X-ray structure of a ClC chloride channel at 3.0 A reveals the molecular basis of anion selectivity. *Nature* 415:287-94.

Elmore, D. E., and D. A. Dougherty. 2001. Molecular dynamics simulations of wild-type and mutant forms of the *Mycobacterium tuberculosis* MscL channel. *Biophys. J.* 81:1345-1359.

Elmore, D. E., and D. A. Dougherty. 2003. Investigating lipid composition effects on the mechanosensitive channel of large conductance (MscL) using molecular dynamics simulations. *Biophys. J.* 85:1512-1524.

Faraldo-Gomez, J. D., G. R. Smith, and M. S. Sansom. 2002. Setting up and optimization of membrane protein simulations. *Eur Biophys J* 31:217-27.

Hess, B., H. Bekker, H. J. C. Berendsen, and J. G. E. M. Fraaije. 1997. LINCS: A linear constraint solver for molecular simulations. *J. Comp. Chem.* 18:1463-1472.

Hille, B. 2001. *Ion Channels of Excitable Membranes.* Sunderland, CT: Sinauer Associates.

Im, W., S. Seefeld, and B. Roux. 2000. A Grand Canonical Monte Carlo-Brownian dynamics algorithm for simulating ion channels. *Biophys. J.* 79:788-801.

Jiang, Y., A. Lee, J. Chen, V. Ruta, M. Cadene, B. T. Chait, and R. MacKinnon. 2003a. X-ray structure of a voltage-dependent K^+ channel. *Nature* 423:33-41.

Jiang, Y., V. Ruta, J. Chen, A. Lee, and R. MacKinnon. 2003b. The principle of gating charge movement in a voltage-dependent K^+ channel. *Nature* 423:42-48.

Koprowski, P., and A. Kubalski. 2003. C termini of the *Escherichia coli* mechanosensitive ion channel (MscS) move apart upon the channel opening. *J. Biol. Chem.* 278:11237-11245.

Levina, N., S. Tötemeyer, N. R. Stokes, P. Louis, M. A. Jones, and I. R. Booth. 1999. Protection of *Escherichia coli* cells against extreme turgor by activation of MscS and MscL mechanosensitive channels: Identification of genes required for MscS activity. *EMBO J.* 18:1730-1737.

Lindahl, E., B. Hess, and D. van der Spoel. 2001. GROMACS 3.0: A package for molecular simulation and trajectory analysis. *J. Mol. Mod.* 7:306-317.

Martinac, B., M. Buechner, A. Delcour, J. Adler, and C. Kung. 1987. Pressure-sensitive ion channel in *Escherichia coli*. *Proc. Natl. Acad. Sci. USA* 84:2297-2301.

Maurer, J. A., and D. A. Dougherty. 2001. A high-throughput screen for MscL channel activity and mutational phenotyping. *Biochim. Biophys. Acta* 1514:165-9.

Miller, S., W. Bartlett, S. Chandrasekaran, S. Simpson, M. Edwards, and I. R. Booth. 2003a. Domain organization of the MscS mechanosensitive channel of *Escherichia coli*. *EMBO J.* 22:36-46.

Miller, S., M. D. Edwards, C. Ozdemir, and I. R. Booth. 2003b. The closed structure of the MscS mechanosensitive channel. Cross-linking of single cysteine mutants. *J Biol Chem* 278:32246-50.

Miyamoto, S., and P. A. Kollman. 1992. SETTLE: An analytical version of the SHAKE and RATTLE algorithms for rigid water models. *J. Comp. Chem.* 13:952-962.

Robertson, K. M., and D. P. Tieleman. 2002. The molecular basis of voltage gating of OmpF porin. *Biochem. Cell Biol.* 80:517-523.

Sanner, M. F., J.-C. Spehner, and A. J. Olson. 1996. Reduced surface: An efficeint way to computer molecular surfaces. *Biopolymers* 38:305-320.

Sayle, R., and E. J. Milner-White. 1995. RasMol: Biomolecular graphics for all. *TIBS* 20:374-376.

Smart, O. S., J. Breed, G. R. Smith, and M. S. P. Sansom. 1997. A novel method for structure-based predictions of ion channel conductance properties. *Biophys. J.* 72:1109-1126.

Sukharev, S. 2002. Purification of the small mechanosensitive channel of *Escherichia coli* (MscS): the subunit structure, conduction, and gating characteristics in liposomes. *Biophys. J.* 83:290-8.

Tieleman, D. P., H. J. C. Berendsen, and M. S. P. Sansom. 2001. Voltage-dependent insertion of a channel forming peptide: Molecular dynamics simulations of alamethicin at phospholipid-water and octane/water interfaces. *Biophys. J.* 80:331-346.

Tieleman, D. P., M. S. P. Sansom, and H. J. C. Berendsen. 1999. Alamethicin helices in a bilayer and in solution: Molecular dynamics simulations. *Biophys. J.* 76:40-49.